nature portfolio

https://doi.org/10.1038/s41893-021-00789-1

## Supplementary information

# On-device lead-absorbing tapes for sustainable perovskite solar cells

In the format provided by the authors and unedited

**Supplementary Information**

# On-device lead absorbing tapes for sustainable perovskite solar cells

Xun Li,[1†] Fei Zhang,[2†] Jianxin Wang, [1] Jinhui Tong, [2] Tao Xu,[1*] Kai Zhu,[2*]

[1]Department of Chemistry and Biochemistry, Northern Illinois University, DeKalb, IL 60115, USA

[2]Chemistry and Nanoscience Center, National Renewable Energy Laboratory, Golden, CO 80401, USA

* Corresponding authors: Kai.Zhu@nrel.gov (K.Z.); txu@niu.edu (T.X.)

† These authors contributed equally to this work.

**Supplementary Figures**

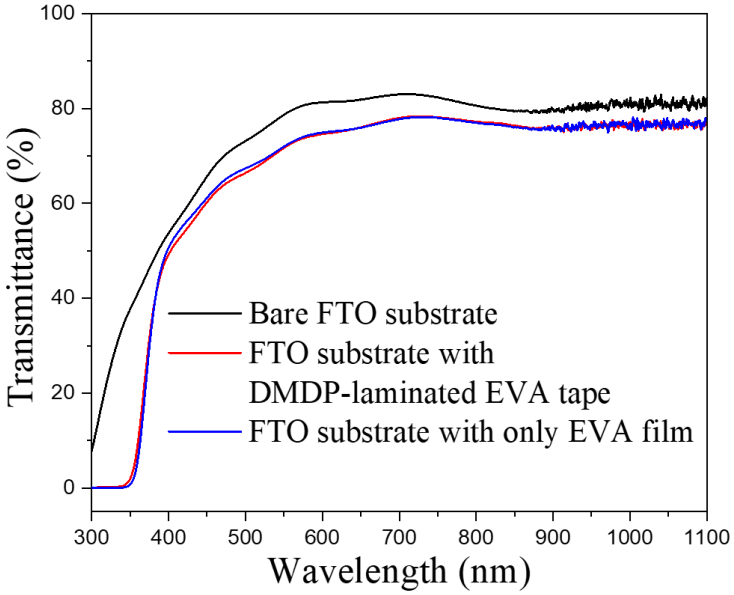


**Supplementary Figure 1.** The optical transmittance of bare FTO glass, FTO glass with only EVA film, FTO galss with DMDP-laminated EVA tape.

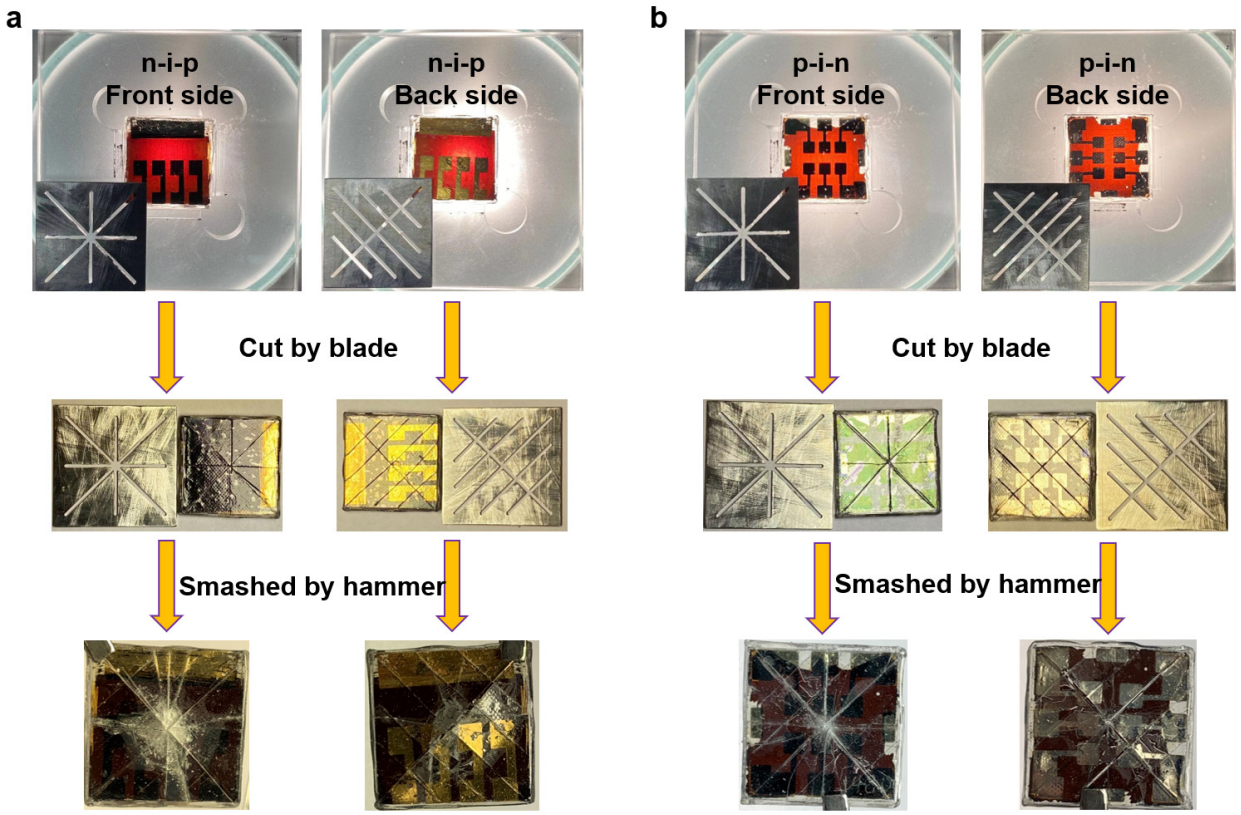


**Supplementary Figure 2.** Illustration of the standardized damaging method for a n-i-p PSC (a) and a p-i-n (b) PSC encapsulated by DMDP-laminated EVA tapes, respectively. Encapsulated PSCs in the sample holder was cut with the guidance of cutting masks for front and back sides, followed by smashing TCO glass substrates by a hammer.

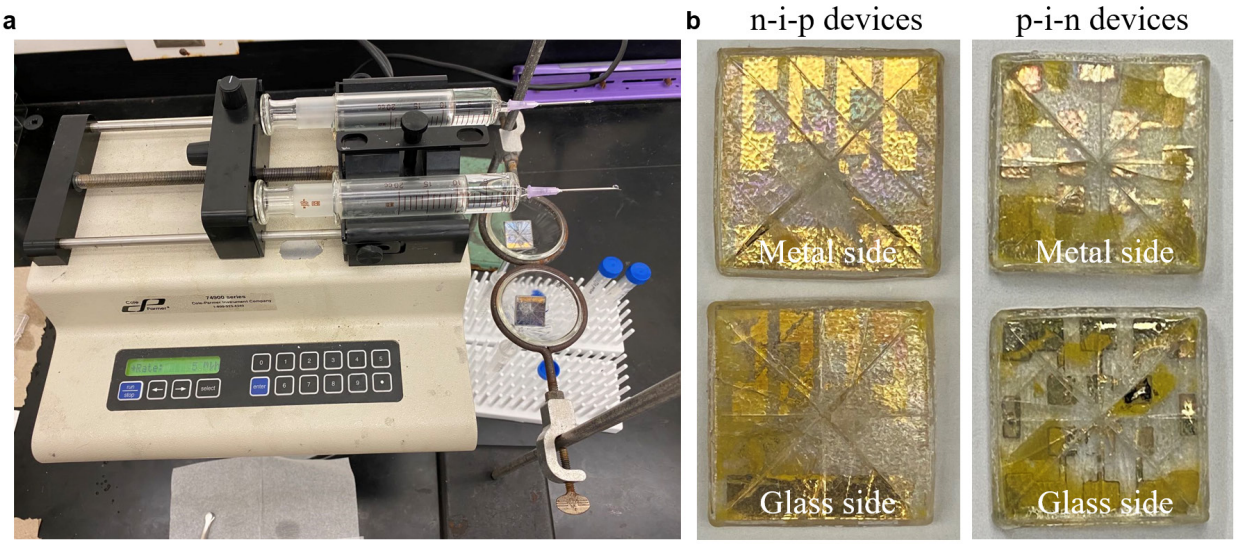


**Supplementary Figure 3. a**, Photograph of water dripping test. Damaged devices were exposed to flow water supplied by a syringe pump to simulate rainfall conditions. **b**, Photographs of encapsulated n-i-p devices (left) and p-i-n devices (right) after water-dripping tests.

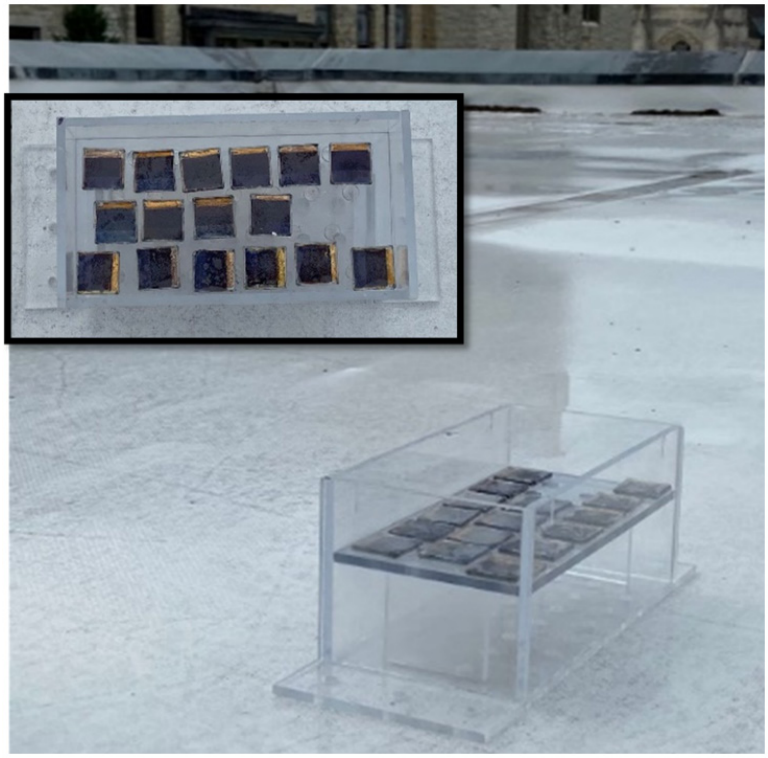

**Supplementary Figure 4.** Photographs of outdoor exposure of encapsulated PSCs in different configurations on a rooftop. The detailed local weather conditions during the outdoor test period (July 15, 2021 to October 15, 2021) can be assessed at https://www.wunderground.com/history/monthly/us/il/rockford/KRFD/date/2020-10.

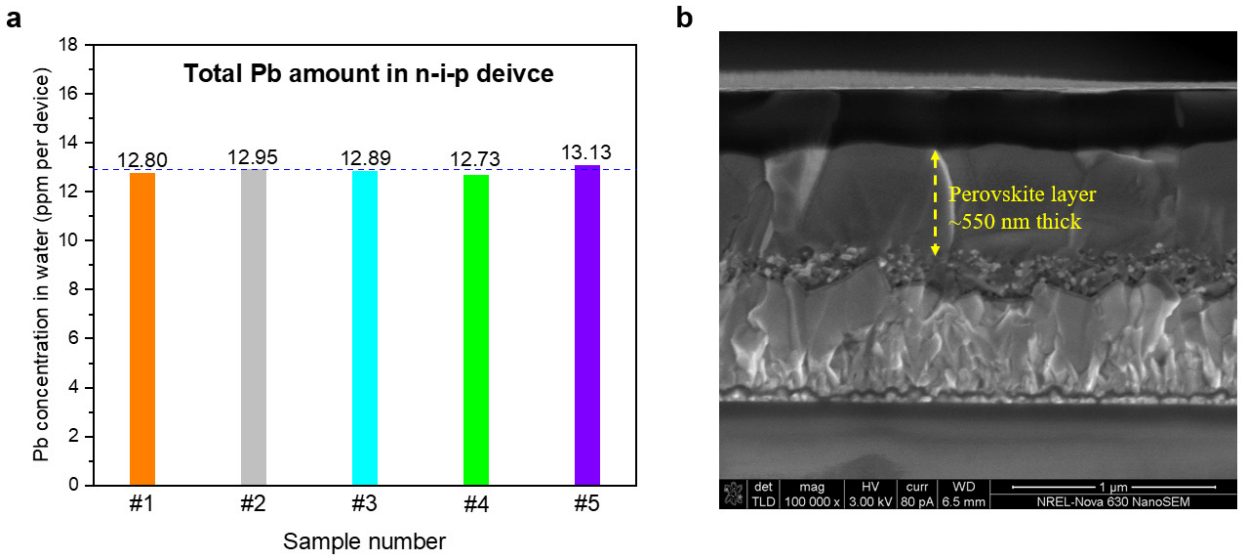


**Supplementary Figure 5. a**, Pb concentration of five n-i-p devices soaked in 40 ml water after 3-month outdoor exposure test. **b**, Typical SEM cross-section image of n-i-p PSCs with typical perovskite layer thickness of ~550 nm and composition of $(CsPbI_3)_{0.05}(MAPbBr_3)_{0.15}(FAPbI_3)_{0.85}$. The dash line in (a) indicates the calculated concentration of $Pb^{2+}$ in a n-i-p PSC when dissolved in 40 ml water. For the perovskite composition $(CsPbI_3)_{0.05}(MAPbBr_3)_{0.15}(FAPbI_3)_{0.85}$, the mass percentage of Pb is 33.7% and the density is ~4.12 g/cm$^3$ calculated from the weighted average of a mixture of $MAPbBr_3$ (density=3.83 g/cm$^3$), $FAPbI_3$ (density=4.10 g/cm$^3$), and $CsPbI_3$ (density=5.39 g/cm$^3$)[1,2]. The total amount of $Pb^{2+}$ in the perovskite layer can be estimated using the density and volume of the perovskite layer along with the mass percentage of $Pb^{2+}$ in the perovskite. Following this approach, we calculated about 12.9 ppm of $Pb^{2+}$ when dissolved in 40 ml water.

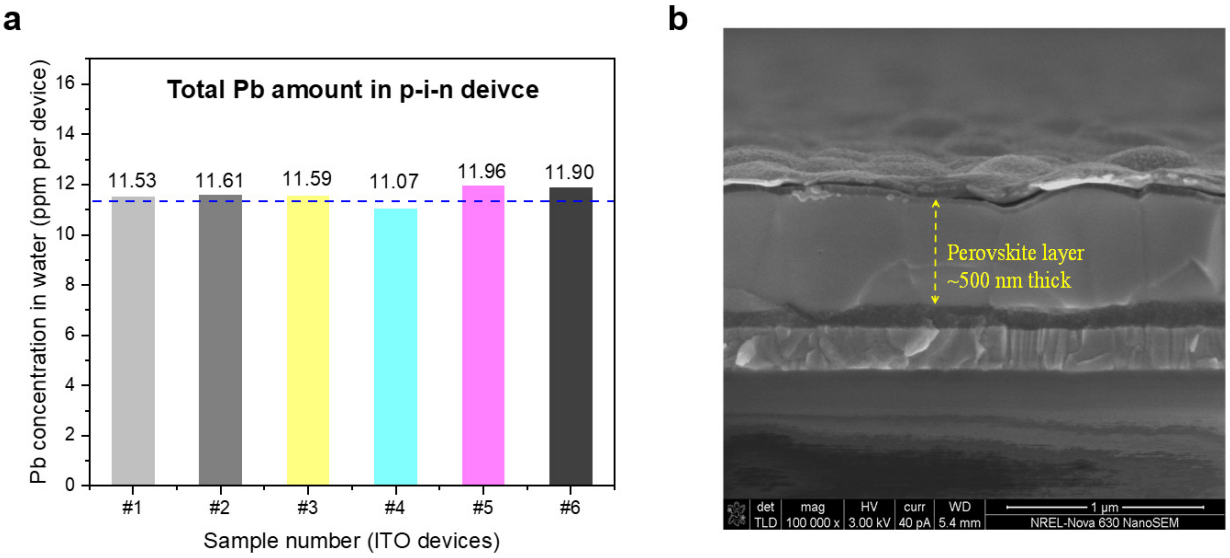


**Supplementary Figure 6. a**, Pb concentration of six p-i-n devices dissolving in 40 ml water. **b**, Typical SEM cross-section image of p-i-n PSCs with typical perovskite layer thickness of ~500 nm and composition of $(CsPbI_3)_{0.05}(MAPbBr_3)_{0.15}(FAPbI_3)_{0.8}$. The dash line in (a) indicates the calculated concentration of $Pb^{2+}$ (about 11.3 ppm) in a p-i-n PSC when dissolved in 40 ml water.

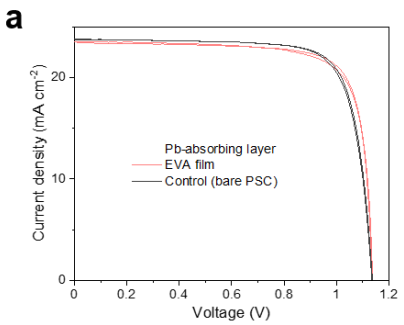


b

| Sample | $V_{oc}$ (V) | $J_{sc}$ (mA cm$^{-2}$) | FF | PCE (%) |
|---|---|---|---|---|
| Control (backward) | 1.138 | 23.80 | 0.769 | 20.83 |
| Control (forward) | 1.139 | 23.75 | 0.778 | 21.05 |
| EVA film (backward) | 1.136 | 23.53 | 0.775 | 20.72 |
| EVA film (forward) | 1.136 | 23.51 | 0.785 | 20.97 |

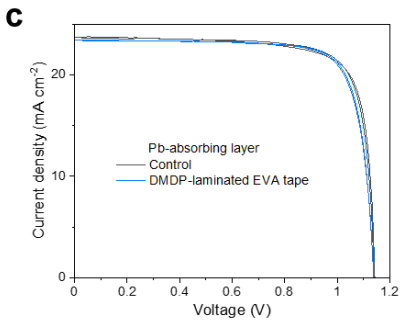


d

| Sample | $V_{oc}$ (V) | $J_{sc}$ (mA cm$^{-2}$) | FF | PCE (%) |
|---|---|---|---|---|
| Control (backward) | 1.143 | 23.75 | 0.780 | 21.17 |
| Control (forward) | 1.141 | 23.68 | 0.789 | 21.31 |
| DMDP-laminated EVA tape (backward) | 1.140 | 23.47 | 0.788 | 21.08 |
| DMDP-laminated EVA tape (forward) | 1.139 | 23.43 | 0.795 | 21.22 |

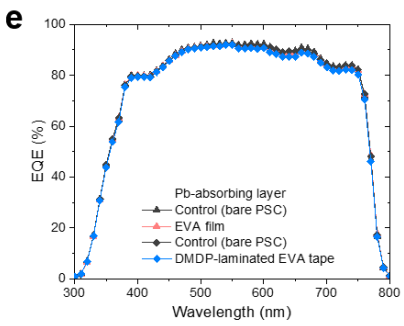


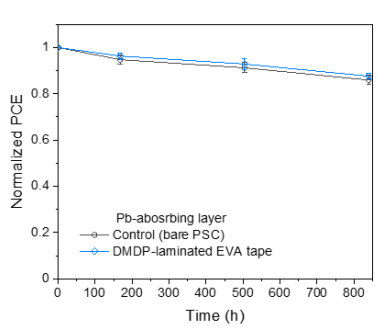


**Supplementary Figure 7. a-d**, Comparison of the J-V characteristics between bare PSC and PSC encapsulated by bare EVA film (a) as well as PSC encapsulated by DMDP-laminated EVA tape (c). b and d are the detailed devices photovoltaic parameters from both backward and forward J-V curves of (a) and (c), respectively, in terms of open-circuit voltage ($V_{oc}$), short-circuit current density ($J_{sc}$), fill factor (FF), and power conversion efficiency (PCE). **e**, Comparison of EQE spectra for PSCs without and with encapsulations. Note that the loss of transmittance in EVA-on-FTO glass with respect to bare FTO glass measured in Supplymentary Fig. 1 is mainly due to total internal reflection at glass-air interface caused by the roughness of EVA tape that scatters the incident light away from surface normal. However, in the EQE measurement, the layer adjacent to FTO glass is the perovskite layer (instead of air) with a higher refractive index (typically greater than 2.2)[3,4] than that of glass (~1.5). Hence, no total internal reflection occurs at FTO-perovskite interface. **f**, Stability comparison of PSCs, under dark at 55°C in ambient condition (20-35% relative humidity), without encapsulation and with encapsulation of DMDP-laminated EVA tapes.

## Supplementary Methods

### Materials

All the chemicals were used as purchased without further purification unless otherwise noted. DMDP was obtained from Eichrom Technologies. Both FAI and MABr were purcahsed from Greatcell Solar. $PbI_2$ and $PbBr_2$ were purchased from TCI. Spiro-OMeTAD was purchased from Merck Corporation. The titanium diisopropoxide bis(acetylacetonate), tert-butylpyridine, is(trifluoromethanesulfonyl)imide lithium salt, caesium iodide (CsI) were purchased from Sigma-Aldrich. The solar-grade EVA films were from Amazon. The glass substrates with patterns of FTO and ITO were obtained from Advanced Election Technology Co., Ltd. and Thin Film Devices Co., Ltd., respectively.

### Device fabrication

*n-i-p Device Fabrication.* Devices were prepared on conductive fluorine-doped tin oxide (FTO)-coated glass substrates. The substrates were cleaned extensively by deionized water, acetone, and isopropanol. A compact titanium dioxide ($TiO_2$) layer of about 40 nm was deposited by spray pyrolysis of 7-mL 2-propanol solution containing 0.6-mL titanium diisopropoxide bis(acetylacetonate) solution (75% in 2-propanol, Sigma-Aldrich) and 0.4-mL acetylacetone at 450°C in air. On top of this layer, mesoporous titanium dioxide was formed by spin-coating 30-nm-sized nanoparticles (Dyesol 30NRD, Dyesol) diluted in ethanol (1:6 *w*/*w*) at 4,500 rpm for 15 s. The $(CsPbI_3)_{0.05}(MAPbBr_3)_{0.15}(FAPbI_3)_{0.85}$ precursor solution was prepared in a glovebox from a 1.4 M $Pb^{2+}$($PbI_2$ and $PbBr_2$) and in the mixed solvent of DMF and DMSO; the volume ratio of DMF/DMSO is 4:1. The spin-coating procedure was performed by 2,000 rpm for 10 s followed with 6,000 rpm for 30 s. At 15 s before the last spin-coating step, 140 μL of chlorobenzene were pipetted onto the substrate. Thereafter, the substrate was put onto a hotplate for 1 h at 100°C Subsequently, the hole-transporting layer (HTM) was deposited on top of the perovskite by spin coating at 4,000 rpm for 15 s. The spiro-OMeTAD solutions were prepared dissolving the spiro-OMeTAD in 1-mL chlorobenzene at a concentration of 60 mM, with the addition of 30 mM bis(trifluoromethanesulfonyl)imide lithium salt from a stock solution in acetonitrile, 200 mM of tert-butylpyridine. The devices were finalized by thermal evaporation of 100-nm gold.

*p-i-n Device Fabrication.* The pre-patterned ITO glass (15 Ω $sq^{-1}$) was sequentially cleaned using acetone and isopropanol alcohol. The hole transporting layer poly[bis(4-phenyl)(2,4,6-trimethylphenyl)amine (PTAA) (Sigma- Aldrich, 2 mg/mL in isopropanol) were spin-coated on the ITO/glass substrates at 5,000 rpm for 30 s and annealed at 100°C for 10 min. The $(CsPbI_3)_{0.05}(MAPbBr_3)_{0.15}(FAPbI_3)_{0.8}$ perovskite precursor were spin-coated on the ITO/PTAA substrates at 5000 rpm for 30 s. During the spin-coating, 800 μL of diethyl ether (DEE) was dropped onto the spinning substrates. The resulting perovskite films were annealed at 100°C for 10 min. After that, C60 (30 nm)/ bathocuproine (BCP) (6 nm)/Ag (100 nm) were sequentially deposited by thermal evaporation.

**Device PV performance characterization**

Solar cell performance measurements were taken under a simulated AM 1.5G illumination (100 $mW/cm^2$, Oriel Sol3A Class AAA Solar Simulator). The photocurrent density–voltage (*J–V*) characteristics were measured using a Keithley 2400 source meter. The *J–V* curves of all devices were measured by masking the active area with a metal mask of area 0.12 $cm^2$. Both backward-scan and forward-scan curves were measured with a bias step of 10 mV and delay time of 0.05 s. The continuous current and power output were measured using a potentiostat (Princeton Applied Research, Versa STAT MC). External quantum efficiency (EQE) spectra of solar cells were measured using a solar cell quantum-efficiency measurement system (QEX10, PV Measurements).

**$Pb^{2+}$-absorption characterization**

The UV-Vis transmission spectra were conducted with an UV-Vis spectrometer (UV-2600, Shimadzu Scientific Instruments) at a spectral range of 300 to 1100 nm. Outdoor exposure of the encapsulated devices was conducted between July and October of 2020 on the rooftop. The samples were collected after three months for further analysis. The Pb detection in water solutions was conducted by flame atomic absorption spectrophotometry (FAAS) and inductively coupled plasma mass spectrometry (ICP-MS). FAAS was performed with an AA-6200 (Shimadzu Scientific Instruments) and equipped with a Pb lamp as the cathode for radiation source. The resonance line wavelength was set at 217 nm. An acetylene/air flame with a flow ratio of 1:4, lamp current of 12 mA, and a slit of 0.7 nm under the mode of BGC-D2 were applied. The calibration curve was prepared by $PbI_2$ solutions (pure water or 2% $HNO_3$/water) in different concentrations

and referenced as a standard to determine the baseline of aqueous Pb content in different conditions. For low Pb concentrations (<0.1 ppm), ICP-MS was used based on a computer-controlled (QTEGRA software) Thermo iCapQ ICP-MS (Thermo Fisher Scientific, Waltham, MA, USA) operating in STD mode and equipped with an ESI SC-2DX PrepFAST autosampler (Omaha, NE, USA). Nickle skimmer and sample cones were used from Thermo Scientific (part numbers 1311870 and 3600812). The internal standard was added inline using the prepFAST system and consisted of 1 ng/mL of a mixed element solution containing Bi, In, $^{6}$Li, Sc, Tb, Y (IV-ICPMS-71D from Inorganic Ventures). Each sample was acquired using 1 survey run (10 sweeps) and 3 main (peak jumping) runs (40 sweeps). The isotopes selected for analysis were $^{206,207,208}$Pb, and $^{89}$Y, $^{115}$In, $^{159}$Tb, $^{209}$Bi (chosen as internal standards for data interpolation and machine stability). The limit of detection for Pb on ICP-MS is <0.005 ppb. Instrument performance is optimized daily through autotuning followed by verification via a performance report (passing manufacturer specifications).

## References


1 Stoumpos, C. C., Malliakas, C. D. and Kanatzidis, M. G. Semiconducting tin and lead iodide perovskites with organic cations: phase transitions, high mobilities, and near-infrared photoluminescent properties. *Inorg. chem.* **52**, 9019-9038 (2013).

2 Leyden, M. R. *et al.* Methylammonium Lead Bromide Perovskite Light-Emitting Diodes by Chemical Vapor Deposition. *J. Phys. Chem. Lett.* **8**, 3193-3198 (2017).

3 Löper, P. *et al.* Complex Refractive Index Spectra of $CH_3NH_3PbI_3$ Perovskite Thin Films Determined by Spectroscopic Ellipsometry and Spectrophotometry. *J. Phys. Chem. Lett.* **6**, 66-71 (2015).

4 Alias, M. S. *et al.* Optical constants of $CH_3NH_3PbBr_3$ perovskite thin films measured by spectroscopic ellipsometry. *Opt. Express* **24**, 16586-16594 (2016).